Computers and Concrete, Vol. 1, No. 3 (2004) 325-354
DOI: http://dx.doi.org/10.12989/cac.2004.1.3.325

Computational optimisation of a concrete model to simulate membrane action in RC slabs

Khandaker M. A. Hossain†

Department of Civil Engineering, Ryerson University, 350 Victoria Street, Toronto, Ontario, Canada, M5B 2K3

Olubayo O. Olufemi‡

Department of Engineering, University of Aberdeen, Aberdeen AB24 3UE, U.K.
(Received November 13, 2003, Accepted March 26, 2004)

Abstract. Slabs in buildings and bridge decks, which are restrained against lateral displacements at the edges, have ultimate strengths far in excess of those predicted by analytical methods based on yield line theory. The increase in strength has been attributed to membrane action, which is due to the in-plane forces developed at the supports. The benefits of compressive membrane action are usually not taken into account in currently available design methods developed based on plastic flow theories assuming concrete to be a rigid-plastic material. By extending the existing knowledge of compressive membrane action, it is possible to design slabs in building and bridge structures economically with less than normal reinforcement. Recent research on building and bridge structures reflects the importance of membrane action in design. This paper describes the finite element modelling of membrane action in reinforced concrete slabs through optimisation of a simple concrete model. Through a series of parametric studies using the simple concrete model in the finite element simulation of eight fully clamped concrete slabs with significant membrane action, a set of fixed numerical model parameter values is identified and computational conditions established, which would guarantee reliable strength prediction of arbitrary slabs. The reliability of the identified values to simulate membrane action (for prediction purposes) is further verified by the direct simulation of 42 other slabs, which gave an average value of 0.9698 for the ratio of experimental to predicted strengths and a standard deviation of 0.117. A 'deflection factor' is also established for the slabs, relating the predicted peak deflection to experimental values, which, (for the same level of fixity at the supports), can be used for accurate displacement determination. The proposed optimised concrete model and finite element procedure can be used as a tool to simulate membrane action in slabs in building and bridge structures having variable support and loading conditions including fire. Other practical applications of the developed finite element procedure and design process are also discussed.

Keywords: concrete modelling; computational optimisation; finite element; reinforced concrete slab; membrane action.

† Professor
‡ Lecturer

1. Introduction

The ultimate strength of a reinforced concrete slab is affected by its end conditions. Conventional yield line theory developed by Johansen (1962) can be used to provide an upper bound to the failure load if the effects of in-plane forces are neglected. However, if a slab is horizontally restrained, compressive membrane forces develop within the slab and yield line theory underestimates the failure load. The effect of compressive membrane action has been recognized since the first half of the 20th century. However, it was not until 1955 when Ockleston (1955) published the results from load tests on a reinforced concrete building in South Africa that researchers became fully aware of its possible benefits. Ockleston (1955) conducted tests on interior floor slabs in the building and found the ultimate load was significantly greater than both the design load and yield line predictions. He attributed this enhancement to compressive membrane action.

Many researchers have looked into compressive membrane action since 1955. Some of the more notable work was done by Park in the 1960s, while Braestrup (1980) summarises much of the work done in this area. Experimental studies by Powell (1956), Wood (1961), Park (1964), Kirkpatrick, *et al*. (1984) and Rankin, *et al*. (1991) have shown that slabs in buildings and bridge decks, which are restrained against lateral displacements at the edges, have ultimate strengths far in excess of those predicted by analytical methods based on yield line theory. The increase in strength has been attributed to membrane action which is due to the in-plane forces developed at the supports. The two types of membrane actions that could be identified from a typical load-deflection curve are the compressive membrane action at small deflections and tensile membrane at large deflections.

Over the years, the theories developed by researchers have largely been based on plastic flow theories and have required gross assumptions to be made (e.g., assuming the concrete to be a rigid-plastic material). The equations derived by these methods are generally unsuitable for design engineers to use and as a result, the benefits of compressive membrane action are usually not taken into account in design or assessment methods (Alan Hon, *et al*. 2001). While the existence of compressive membrane action is commonly acknowledged, its use in practical situations is hindered by a lack of knowledge of the stiffness of the horizontal restraints and how this effects the development of membrane forces. This surround stiffness is critical to the development of compressive membrane action. Recently, Eyre (1997) has developed a method to directly assess the strength of reinforced concrete slabs under membrane action. The method requires knowledge of the surround stiffness that the slab is exposed to and determines a “safe load” that is always less than the ultimate load.

In recent times comprehensive research has been conducted over wide range of building and bridge structures to understand and to incorporate beneficial effect of membrane action in the structural design (Peel-Cross, *et al*. 1998, Taylor, *et al*. 1998a, 1998b, Rankin, *et al*. 1999, Taylor 2000, Salim and Sebastian 2003, Huang, *et al*. 2003a, 2003b, Salami 1994). Experimental and design-oriented investigations are concentrated on the understanding of membrane action in bridge structures to develop a design method for the ultimate load capacity of bridge deck slabs with a range of boundary conditions (Taylor, *et al*. 1998a, 1998b, Rankin, *et al*. 1999, Taylor 2000). Bridge decks have an inherent strength due to the in-plane membrane forces set up as a result of restraint provided by beams, diaphragms, etc. By utilising the advantages of high strength concrete in laterally restrained beams and by extending the existing knowledge of compressive membrane action, it should be possible to produce bridge decks with less than normal reinforcement. A primary conclusion from this research is that bridge deck slabs have strengths far in excess of those predicted

by conventional design methods, which are based upon flexural theory. This strength enhancement is attributable to compressive membrane action.

More recently, the finite element method has been used to model the membrane action in reinforced concrete slabs (Alan Hon, *et al.* 2001, Huang, *et al.* 2003a, 2003b, Salami 1994). Huang, *et al*. (2003a, 2003b) used the non-linear layered finite element procedure to model the membrane action of concrete slabs in composite buildings under fire conditions. This research was concentrated on solid reinforced concrete slabs with simply supported edges at ambient temperature under uniform loading. This was followed by a simulation of a full-scale fire test on a solid reinforced concrete slab floor at the Cardington Laboratory in UK. It is evident that the proposed model can predict structural behavior of reinforced concrete slabs and their influence on composite steel-framed buildings in fire with good accuracy. In all cases the development of membrane actions is demonstrated, and the structural behavior differs compared with the geometrically linear case. These studies provide evidence that at very high temperatures the floor slab becomes the main load-bearing element, and the floor loads above the fire compartment are carried largely by tensile membrane forces developed mainly in the steel anticracking mesh or reinforcing bars.

The finite element method is capable of analysing membrane action in slabs due to its ability to incorporate both geometric and material nonlinearities in its formulation. The non-linear material models developed for the finite element analysis of concrete structures have hitherto been used, mainly for the simulation of previous experiments or the analysis of existing structures. For many users the parameter values involved in these models vary for each experiment being simulated. Very seldom have these models been used to carry out reliable predictions of structural behaviour especially to model membrane action in slabs in buildings and bridges, (with a set of fixed model parameter values identified for that class of problem). This objective forms the basis of the present paper, focusing on the class of fully clamped slabs where membrane action is prominent.

Implicit in non-linear material models are parameters, some of the values of which are identified directly from simple laboratory tests, while the rest are determined based on the model's ability to simulate previous tests. A simple concrete material model, incorporated in a finite element program, has been the subject of extensive parametric and sensitivity studies, to identify, for fully clamped slabs, a set of fixed parameter values and computational conditions, which would guarantee reliable simulation of membrane action when the model is used in the analysis of arbitrary fully clamped concrete slabs.

Tests carried out by Powell (1956) and Park (1964) on eight fully clamped slabs are used as basis for the basic simulation process and parametric studies, to identify the set of conditions and model parameter values. The reliability of the identified fixed values and computational conditions for prediction purposes is further verified by the direct simulation of 42 other fully clamped slabs, tested by various researchers. The strength predictions for all the slabs are fairly accurate, with an average ratio of 0.9698 established for the ratio of experimental to predicted load values. In the basic simulation process, a factor d_f (the deflection factor), relating the ratio of experimental to predicted deflection is established, which when used in the subsequent direct simulation process, is found to be reasonably accurate, (for slabs with identical degree of fixity), thus showing that such a factor could be used to predict the corresponding peak displacement of arbitrary fully clamped concrete slabs.

The avenues for practical applications of reliable finite element predictions incorporating membrane action in concrete slabs through optmisation of concrete model parameters and numerical conditions are very vast. Literally hundreds of finite element model slabs could be analysed, varying

material and geometric values, and upon this database charts could be developed, which would serve for quick strength and corresponding displacement determination of arbitrary slabs in building and bridge structures.

2. Finite element modelling

The 3D degenerated, layered shell element, having five degrees of freedom at each node is used for spatial discretisation (Owen, *et al*. 1983), and parametric studies were carried out with reduced, selective and full integration schemes. Reinforcing steel is represented with a layer of equivalent thickness, with non-linear uniaxial strength and rigidity properties. Geometric nonlinearity is taken into account using the Total Lagrangian approach.

2.1. Concrete model

A plasticity formulation based concrete material model, capable of responding to both perfectly plastic and strain hardening behaviour is adopted for this study. It incorporates concepts such as the yield criterion, flow and hardening rules, and crushing condition (Owen and Figueiras 1984). A dual criterion for yielding and crushing in terms of stresses and strains is considered, which is complemented with a tension cut-off representation. The yield criterion is assumed to be a modified Drucker Prager surface with a curved meridian, having its parameters determined from Kupfer's (1969) test results, and is expressed in terms of stress components as:

$$f(\sigma) = 2\{1.355[(\sigma_x^2 + \sigma_y^2 - \sigma_x\sigma_y) + 3(\tau_{xy}^2 + \tau_{xz}^2 + \tau_{yz}{}^2)] + 0.355\sigma_o(\sigma_x + \sigma y)\}^{0.5} = \sigma_o \qquad (1)$$

where σ_o is the equivalent effective stress, which for a perfectly plastic model is taken as the ultimate uniaxial compressive strength of concrete f'_c, and for a strain hardening model σ_o is $0.3f'_c$. During loading an elastic response is assumed up to σ_o after which elastic-plastic, or where applicable, a perfectly plastic, behaviour commences until a 'crushing surface', defined in strain space, is reached. This is defined in terms of strain components as:

$$1.355[(\varepsilon_x^2 + \varepsilon_y^2 - \varepsilon_x\varepsilon_y) + 0.75(\gamma_{xy}^2 + \gamma_{xz}^2 + \gamma_{yz}^2)] + 0.355\varepsilon_{cu}(\varepsilon_x + \varepsilon_y) = \varepsilon_{cu}^2 \qquad (2)$$

where ε_{cu} is a specified ultimate compressive strain, which, when reached signifies the loss of all the strength and rigidity of the concrete material. Fig. 1(a) illustrates the one dimensional representation of both the perfectly plastic and the strain-hardening model. The two dimensional representation of the yield surface in the principal stress space is shown in Fig. 1(b). Unloading follows the initial elastic modulus E_o and an elastic response occurs for subsequent loading until the corresponding loading surface is reached. Further loading causes an elasto-plastic response with increasing plastic deformation and a corresponding expansion of the loading surface according to the flow and hardening rules.

2.2. Modelling of tensile behaviour of concrete

The response of concrete under tensile stresses is assumed to be linear elastic until the fracture

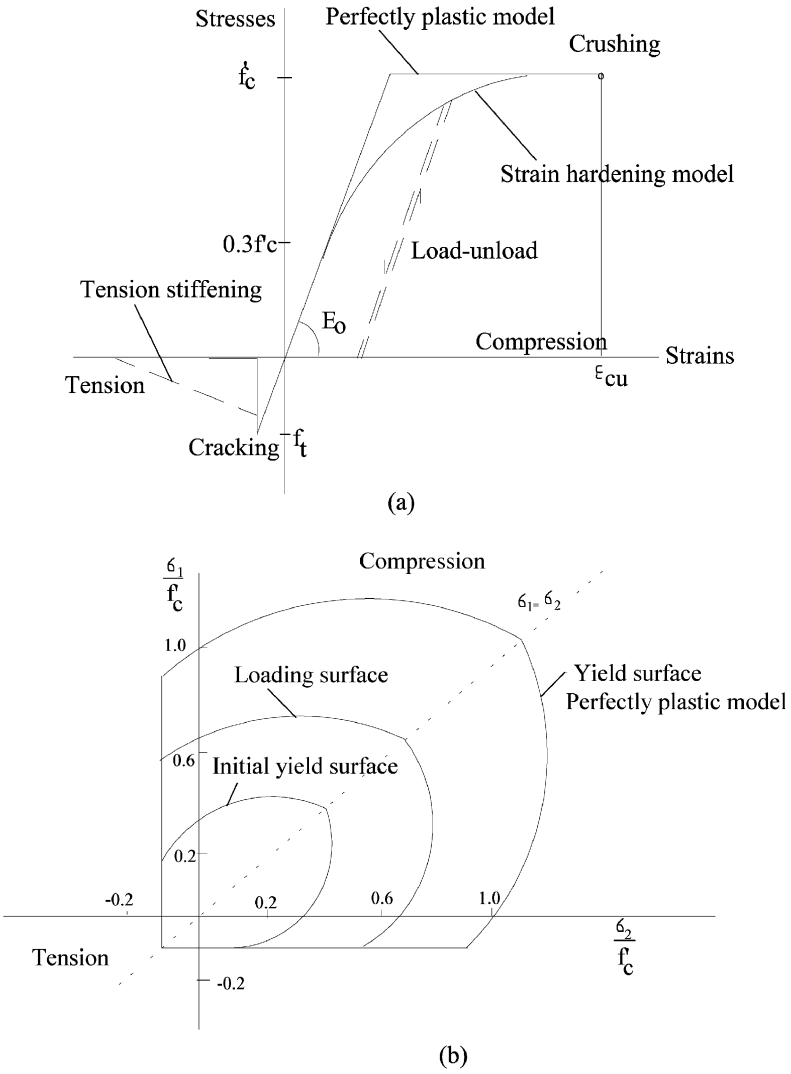

Fig. 1 Representation of the concrete constitutive model

surface is reached and is governed by a maximum tensile stress criterion (tension cut-off). Cracks are assumed to form in planes perpendicular to the direction of maximum principal tensile stress as soon as this reaches the specified concrete tensile strength f'_t. A smeared representation for cracked concrete is assumed, where cracks are distributed across a region of the finite element. As the overall structural behaviour is of primary concern in this study and the size of elements used for analysis are relatively large, the problem of strain localisation that such assumption may cause in a fine mesh situation does not arise. To take account of the effect of tension stiffening due to the presence of reinforcement, a gradual release of the concrete stress component normal to the cracked plane and shown in Fig. 2, is adopted. Unloading and reloading of cracked concrete is assumed to be linear, with a fictitious elasticity modulus E_i defined as:

$$E_i = \alpha f'_t(1-\varepsilon_i/\varepsilon_m)/\varepsilon_i \ldots\ldots\ldots\ldots\ldots \varepsilon_t \le \varepsilon_i \le \varepsilon_m \tag{3}$$

where α and ε_m, are tension stiffening parameters and ε_i is the maximum value of tensile strain at the point considered. The normal stress σ_1 is obtained by the expressions:

$$\begin{aligned} \sigma_1 &= \alpha f'_t(1-\varepsilon_1/\varepsilon_m), \ldots\ldots\ldots\ldots \varepsilon_t \le \varepsilon_1 \le \varepsilon_m \ldots \text{ or by:} \\ \sigma_1 &= \sigma_i \varepsilon_1/\varepsilon_i \ldots\ldots\ldots\ldots\ldots \text{if } \ldots \varepsilon_1 < \varepsilon_i \end{aligned} \tag{4}$$

where ε_1 is the current tensile strain in material direction 1. The value of f'_t is taken as the modulus of rupture, f_r of the concrete and can be related to the uniaxial compression strength (in MPa) by : $f_r = 0.62(f'_c)^{0.5}$. An appropriate value of cracked shear modulus based on the approach of Cedolin, *et al.* (1977), which is a function of the current tensile strain, is employed to account for aggregate interlock and dowel action in the smeared crack model. This allows for shear transfer across the rough surface of the cracked concrete.

2.3. Modelling of steel behaviour

The reinforcement bars are modelled as layers of equivalent thickness (Owen and Figueiras 1983) and follows an elastoplastic material behaviour, with the Von Mises yield criterion defining the yield surface (Owen and Hinton 1980).

3. Preliminary computational studies

Eight reinforced concrete slabs tested by Powell (1956) and Park (1964) are used as basis for the preliminary finite element simulation and subsequent parametric studies. All the slabs are fixed against displacements and rotations along their edges and a uniformly distributed load is applied on the surface. The successful simulation of the behaviour of these slabs in the parametric studies,

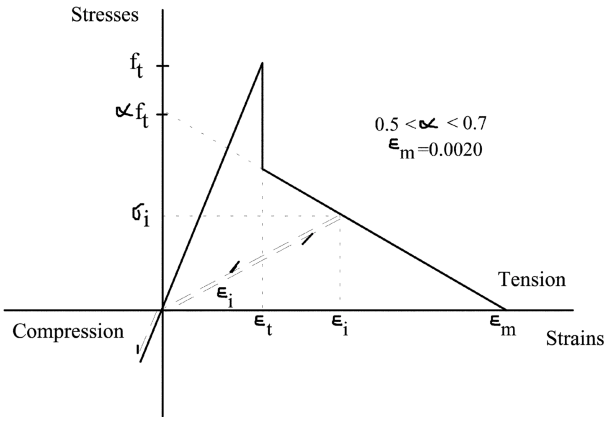

Fig. 2 Tension stiffening in cracked concrete

would lead to the identification of a set of optimised parameter values and computational conditions, which would guarantee reliable predictions in subsequent analyses.

3.1. Slab details

Powell's (1956) four slabs ($914.4 \times 522.5 \times 32.7$ mm) are isotropically reinforced at the top and bottom layers. The reinforcement extends to the full length of the slab and the percentage of steel is calculated on the basis of the mean effective depth (d). Table 1 gives a summary of the test slabs where L_x and L_y are lengths of the short and long sides of the slab, respectively and h represents the total depth.

Park's (1964) four series A slabs ($1524 \times 1016 \times 50.8$ mm) are reinforced anisotropically, with the bottom steel extending over the whole length, while the top steel extends into the slab from the edges, over a distance calculated by yield line theory. The full details of Park's slabs are also summarised in Table 1. The percentage of steel is calculated on the basis of actual effective depth.

3.2. Finite element idealisation

The slabs were idealised with 3D degenerated, 8-noded shell elements, having five degrees of freedom at each node. A symmetric quarter of each slab was discretised into eight finite elements. The detailed finite element descretisation with reinforcement pattern for the slabs are as shown in Figs. 3(a-c). The concrete depth is discretised into 10 layers of equal thickness. The details of the idealisation of the concrete and steel layers are as shown in Fig. 3(c).

3.3. Displacement control (DC) and load control (LC) strategies

The simulations were carried out based on both displacement control (DC**)** and load control (LC**)** strategies. In DC, prescribed displacements reflecting the deflected shape of the slabs under uniformly distributed loading conditions, are applied incrementally to simulate the complete load-

Table 1 Detailed description of fully clamped slabs

Slab No.	L_y/L_x	L_x/h	% of Steel Reinforcement				f_y N/mm^2	f'_c N/mm^2
			Short span		Long span			
			Top	Bottom	Top	Bottom		
Powell's Slabs (1956)								
S50	1.75	16	0.45	0.45	0.45	0.45	211	37.2
S54	〃	〃	0.71	0.71	0.71	0.71	211	41.0
S59	〃	〃	0.97	0.97	0.97	0.97	255.2	39.3
S63	〃	〃	1.53	1.53	1.53	1.53	255.2	41.0
Park's Slabs (1964)								
A1	1.50	20	0.38	0.19	0.41	0.20	327.6	33.0
A2	〃	〃	0.84	0.42	0.43	0.21	327.6	29.5
A3	〃	〃	1.44	0.72	0.45	0.22	327.6	34.4
A4	〃	〃	2.42	1.21	0.47	0.23	327.6	27.7

f'_c: Concrete cylinder strength; f_y: Yield strength of steel

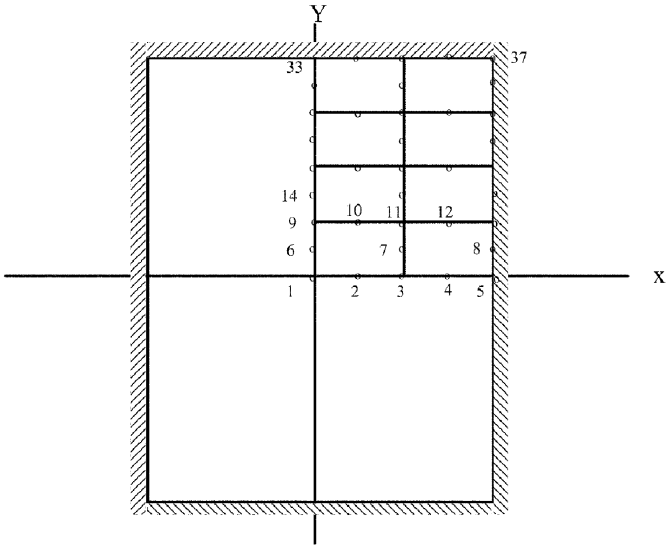

Fig. 3(a) Typical slab finite element mesh

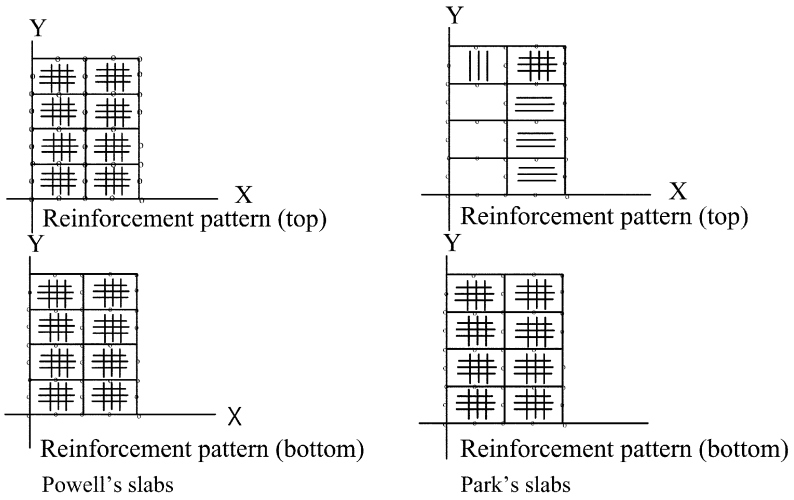

Fig. 3(b) Typical Finite element reinforcement pattern for the slabs

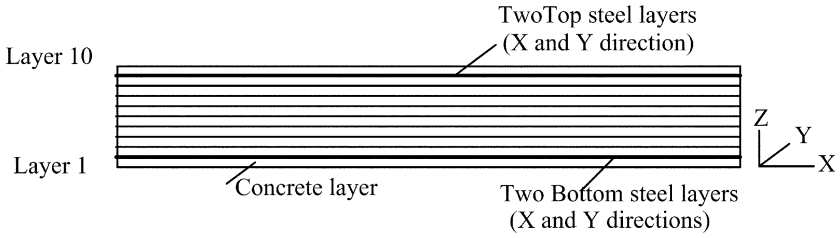

Fig. 3(c) Discretisation of steel and concrete layers

deflection responses. In LC, uniformly distributed loads were directly applied on the slabs incrementally and a peak load, associated with a sudden large deflection, can be identified from the finite element solutions. The typical finite element load-deflection responses from DC and LC are superimposed to that from a typical experiment in Fig. 4. A relationship is established between the finite element peak deflection (d_{fe}) and experimental peak deflection (d_{exp}), via a deflection factor (d_f) such that; $d_{exp} = d_{fe} \times d_f$.

3.4. Parametric studies for optimisation of model parameters

A series of comprehensive parametric studies have been carried out to establish the sensitivity of various model parameters and computational conditions involved in the finite element modelling. These are the convergence criteria, integration rules, non-linear solution techniques, ultimate compressive strain of concrete (ε_{cu}), tension stiffening parameters α and ε_m, modulus of elasticity of concrete (E_c) and the elasto-plastic modulus of steel (E'_s).

3.4.1. Effect of convergence criteria

Convergence criteria either based on force norm or displacement norm seems to have no influence on the load deflection response in the pre-peak stages as can be seen from Fig. 5(a). However in the post-peak stages, there are some differences in the rising and falling branches of the curve but the over all trend seems to be the same. The CPU time required in the run using force norm as convergence criteria is almost 10 times higher than that required in the runs using displacement norm.

3.4.2. Effect of integration rules and non-linear solution process

Parametric studies were conducted with initial stiffness (IS), tangential stiffness (TS), Newton-Raphson (NR) and modified Newton-Raphson (MNR) nonlinear solution processes. The load-deflection response is found to be dependent on the selection of integration rules and non-linear solution process. It is evident from Figs. 5(b-d) that the selective integration (SI) seems to simulate better load-deflection response than normal (NI) and reduced (RI) integration's. The NI resulted in the worst post peak response. Considering the peak load, the RI is unable to produce a single peak despite the fact that it produces a series of close peaks after the first peak. The RI also produces higher first peak loads and corresponding peak deflections. Considering overall response, SI seems

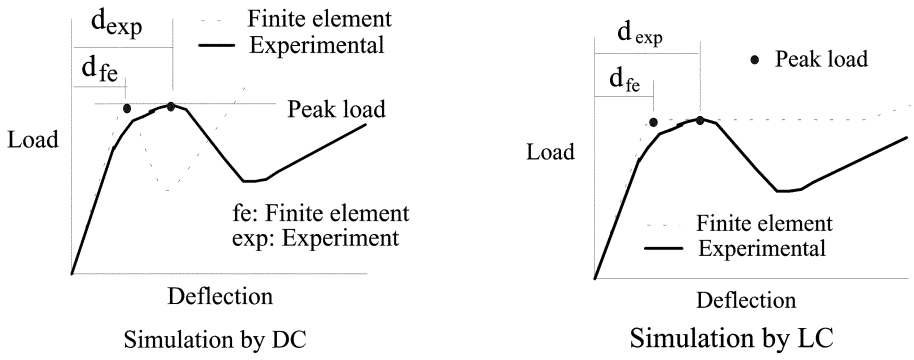

Fig. 4 Load-deflection response of fully clamped slabs with membrane action

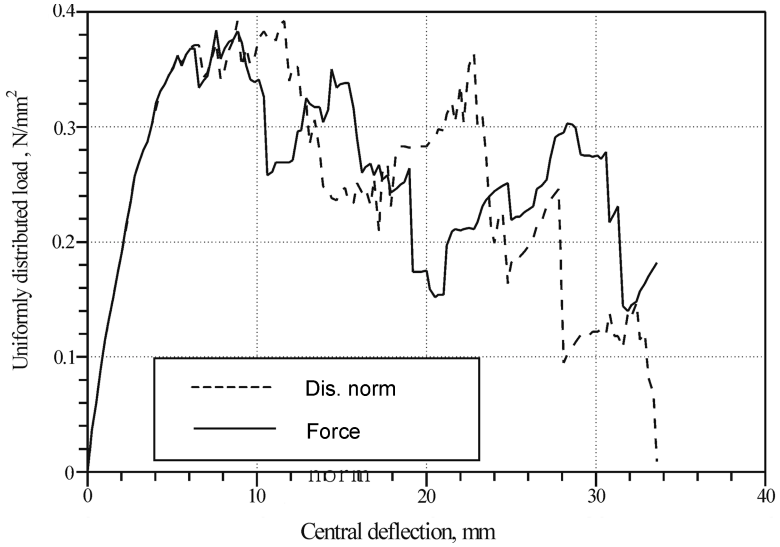

Fig. 5(a) Effect of convergence criteria

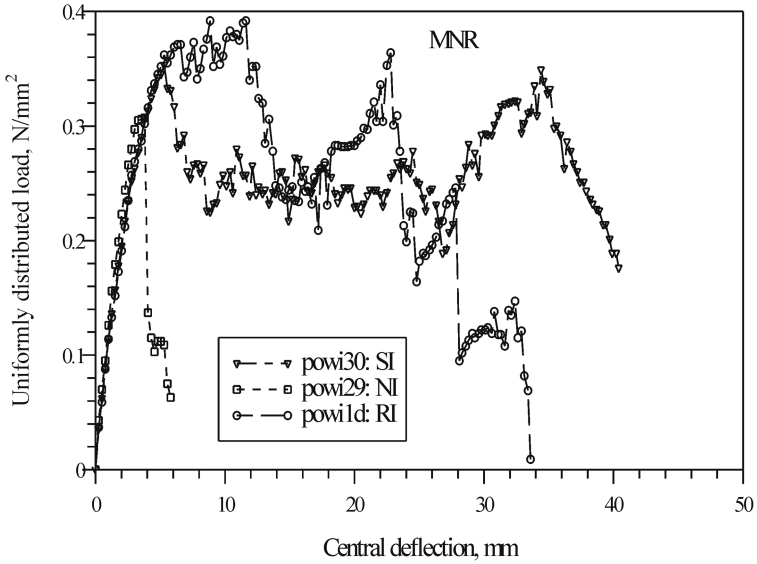

Fig. 5(b) Effect of integration rules and solution processes

to provide a better response than those of the others although it needs more CPU time than RI.

Comparing Figs. 5(b-d), the SI with initial stiffness (IS) seems to result in the better load-deflection response. Table 2 is compiled to provide a summary of the effect of integration rules and non-linear solution processes on the simulation of load-deflection response. The IS method produces a slightly higher peak load with similar deflection compared to others with much less CPU time. It was therefore decided to carry out the simulation with the combination of SI and IS.

Table 2 Results of parametric studies

Influence of solution process and integration schemes									
Solution process	SI			RI			NI		
	P.load	P.def.	CPU	P.load	P.def.	CPU	P.load	P.def.	CPU
MNR	0.353	5.31	4861	0.37	6.57	3361	0.307	3.79	----*
NR	0.354	5.30	----*	0.375	6.32	----*	0.307	3.54	3848
TS	0.354	5.31	7698	0.371	6.32	4104	0.306	3.54	8026
IS	0.36	5.30	653	0.404	6.57	319	0.326	4.04	677

Influence of ε_m				
ε_m	ε_{cu} = 0.006		ε_{cu} = 0.0035	
	P.load N/mm^2	P.def. mm	P.load N/mm^2	P. def. mm
0.002	0.36	5.30	0.267	3.04
0.003	0.362	5.31	0.268	3.03
0.004	0.363	5.31	0.269	3.03

*Run terminates before the given number of load incremetns

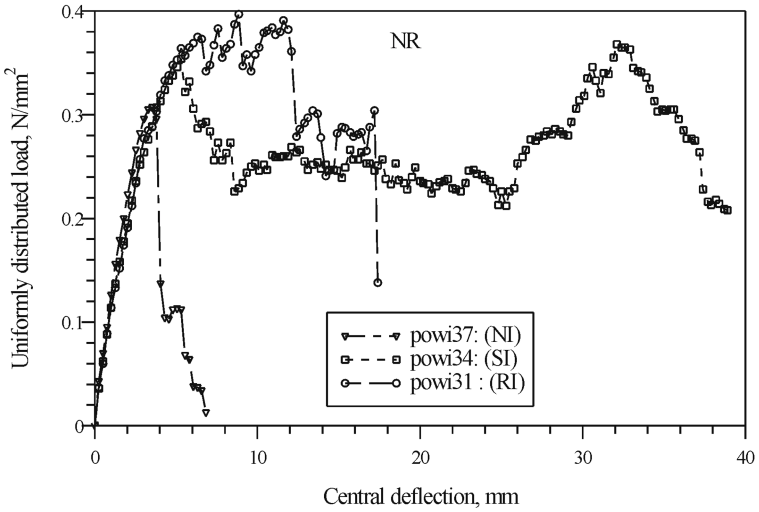

Fig. 5(c) Effect of integration rules and solution processes

3.4.3. Effect of ultimate compressive strain of concrete (ε_{cu})

The ε_{cu} is found to be the most important concrete material parameter which controls the load and deflection in the numerical simulation of the slabs using the non-linear finite element program employing layered shell elements. The peak load and corresponding deflection were found to be sensitive to the change in the value of ε_{cu}. The peak load and corresponding peak deflections increased with the increase of ε_{cu} is illustrated in Fig. 5(e) An increase of ε_{cu} from 0.0035 to 0.0055 increased the load by 1.36 times and the corresponding deflection by 1.48 times.

3.4.4. Effect of tension stiffening parameter ε_m

The effect of ε_m on the load-deflection response with various combinations of ε_{cu} is presented in

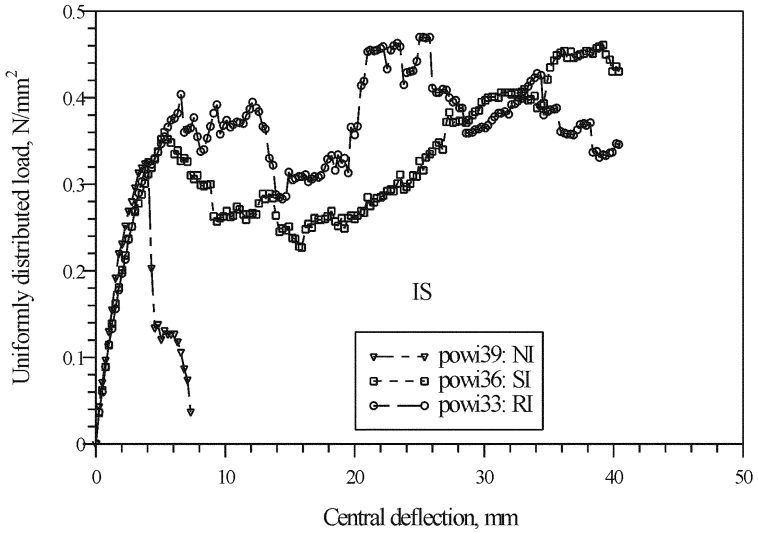

Fig. 5(d) Effect of integration rules and solution processes

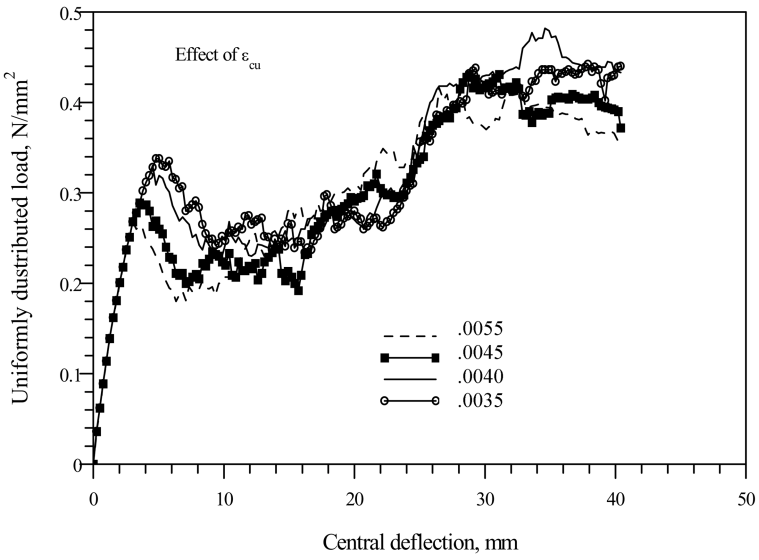

Fig. 5(e) Effect of ε_{cu}

Fig. 5(f) and illustrated in Table 2. The overall load-deflection response seems to be not affected with the change of ε_m. For a constant value of $\varepsilon_{cu,}$ ε_m has no effect on the first peak load and correspond-ing peak deflection.

3.4.5. Effect of modulus of elasticity of concrete (E_c)

An increase in E_c, increased the peak load with a slight decrease in peak deflection and has no effect on the general load-deflection response (Fig. 5(g)).

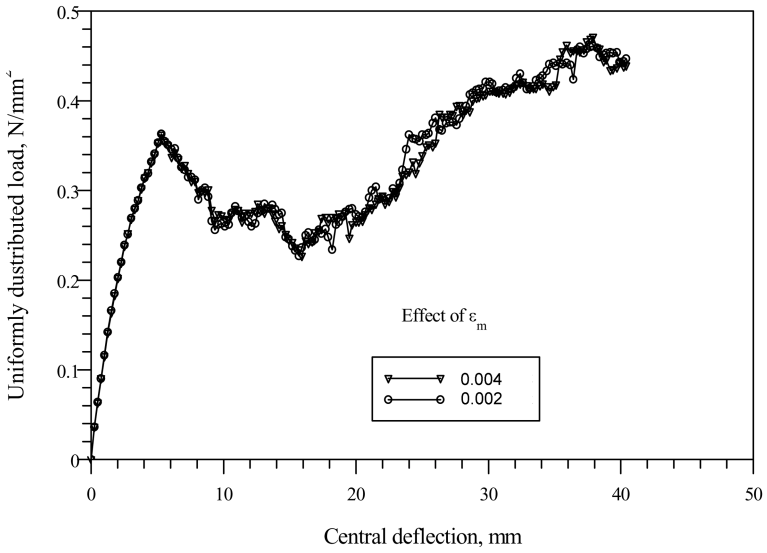

Fig. 5(f) Effect of ε_m

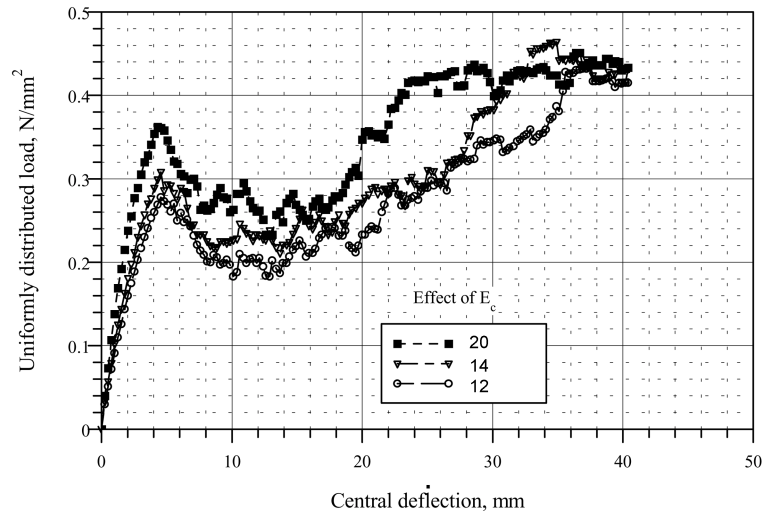

Fig. 5(g) Effect of E_c on load-deflection response

3.4.6. Effect of tension stiffening parameter α

The effect of α is plotted in Fig. 5(h). The general load-deflection response remains similar and the peak load and corresponding peak deflection are found to be not sensitive to the change in the value of α. A value of 0.5 for α will be adequate for simulation.

3.4.7. Effect of elasto-plastic Young's modulus of steel (E'_s)

The post peak response is found to be affected with the change of E'_s (Fig. 5(i)). The peak load tends to increase with increase of E'_s but peak deflection seems to be not affected.

The single parameter to which the slab simulation is most sensitive, and which can be adjusted to

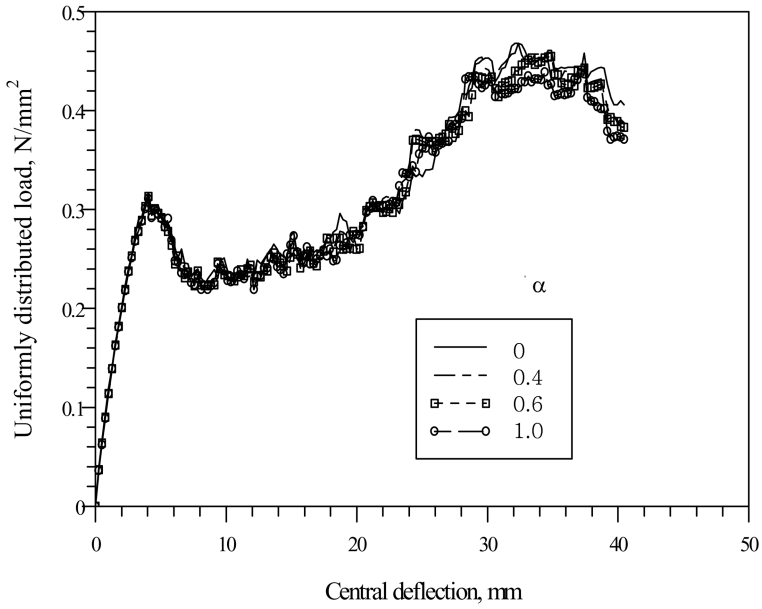

Fig. 5(h) Effect of α on the load-deflection response

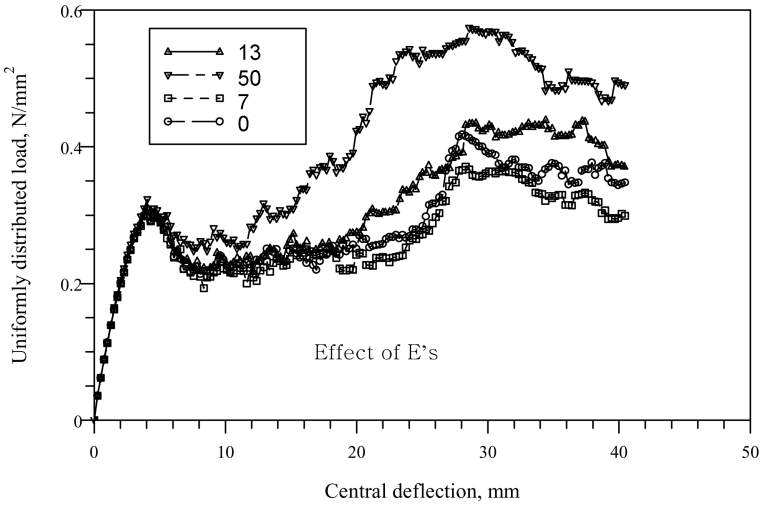

Fig. 5(i) Effect of E'_s on the simulation

achieve accurate simulation while the other parameters are fixed, is the ultimate concrete crushing strain ε_{cu}. Study has shown that the value of ε_{cu} required for reliable simulation is dependent on the slab support conditions, which also delineates the class of problem. The other computational conditions established from the preliminary study, and which are adopted for the simulation are as follows: selective integration scheme (SI), initial stiffness method (IS), and convergence criterion based on displacement norm (DN). Actual test values were chosen for material properties such as the Young's moduli for the steel and concrete, (E_s & E_c), and the yield strengths of concrete and

steel, (f'_c & f_y). The fixed values chosen for the other parameters are, for the tension stiffening parameters, (α : 0.5, ε_m: 0.002), and the elastoplastic modulus for steel, E'_s is E_s/15, where E_s is the steel Young's modulus. The Poisson ratios for concrete and steel are chosen as 0.18 and 0.25 respectively.

4. Basic simulation

The typical finite element load-displacement responses of Powell's and Park's slabs, based on the displacement control (DC) strategy for various values of ε_{cu}, are superimposed on test results and shown in Figs. 6(a - d), and also summarised in Table 3. The corresponding results based on the load control (LC) strategy are shown in Figs. 7(a - d) and summarised in Table 3.

From Table 3, it is seen that Powell's fully clamped slabs with isotropic reinforcement can be

Table 3 Comparison between DC and LC simulations with Powell's (1956) experiment

Slab No.	Experiment Load*	Defl. (mm)	F.E. (**DC**) Load*	Defl. (mm)	**Ratio**# Expt/FE Load	Defl.	F.E. (**LC**) Load*	Defl. (mm)	Ratio# Expt/FE Load	Defl.
S50	0.33	10.76	0.33	4.55	1.00	2.36	0.32	3.36	1.03	3.20
S54	0.36	10.38	0.345	4.28	1.04	2.42	0.37	3.40	0.973	3.05
S59	0.35	13.63	0.354	4.04	0.99	3.37	0.39	3.55	0.90	3.84
S63	0.464	10.80	0.42	4.55	1.10	2.37	0.51	3.36	0.91	3.21
			ε_{cu}= 0.0045		1.026	2.37	ε_{cu}= 0.0025		0.953	3.32
			d_f =2.37		Mean values		d_f =3.32		Mean values	

*Load (in N/mm^2) # Ratio of experimental to finite element values

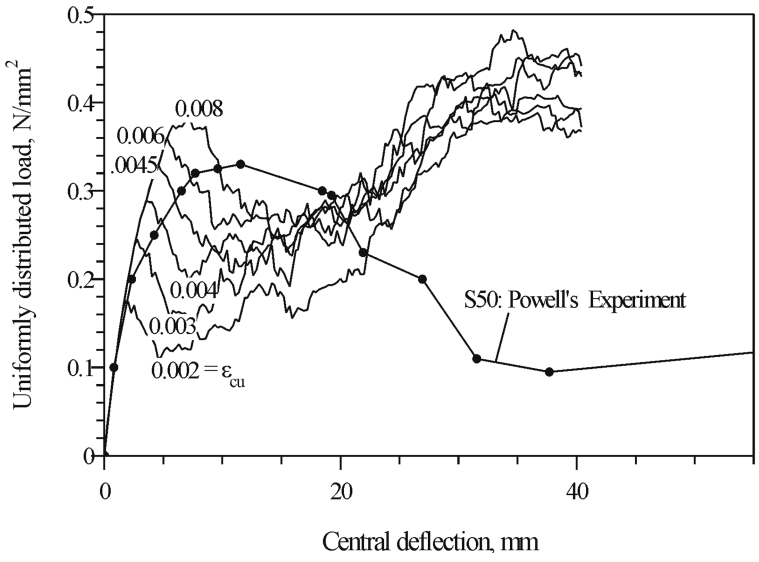

Fig. 6(a) Simulation of Powell's slab S50 under DC

simulated by adopting an ε_{cu} value of 0.0045 in a DC strategy and 0.0025 for the case of LC. The ratio of experimental to predicted load averages at 1.026 for DC and 0.94 for LC, showing a fairly good level of agreement. Park's fully clamped slabs with anisotropic reinforcement, simulated with ε_{cu} values of 0.0035 and 0.004 in the case of DC, and an ε_{cu} value of 0.0025 in the case of LC, are summarised in Tables 4(a) & 4(b) respectively. The ratio of experimental to predicted load averages at 0.87 (for ε_{cu}=0.004) and 0.953 (for ε_{cu}=0.0035) for the DC strategy, and 1.02 for LC strategy, showing reasonably good agreement.

For simulations carried out on the basis of load control (LC) strategy, a single value of ε_{cu} (i.e., 0.0025) can be used for both Powell and Park's slabs, but for the case of DC simulation, a higher value of ε_{cu} is required in the simulation of Powell's slabs, in order to obtain acceptable results.

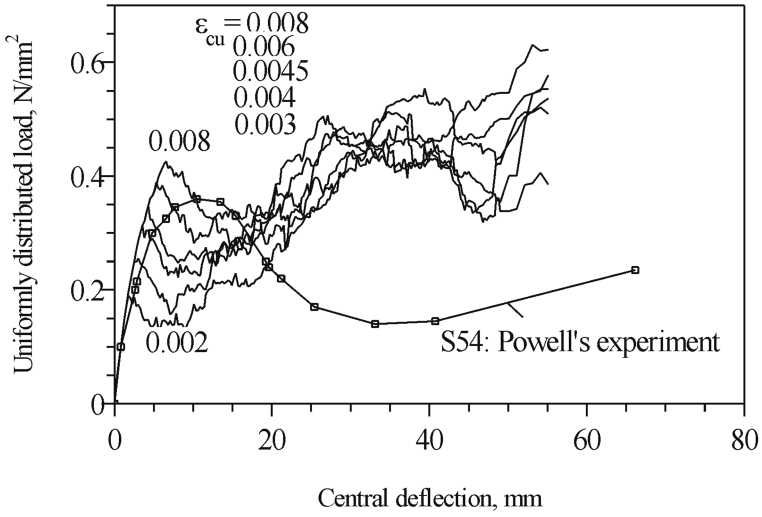

Fig. 6(b) Simulation of Powell's slab S54 under DC

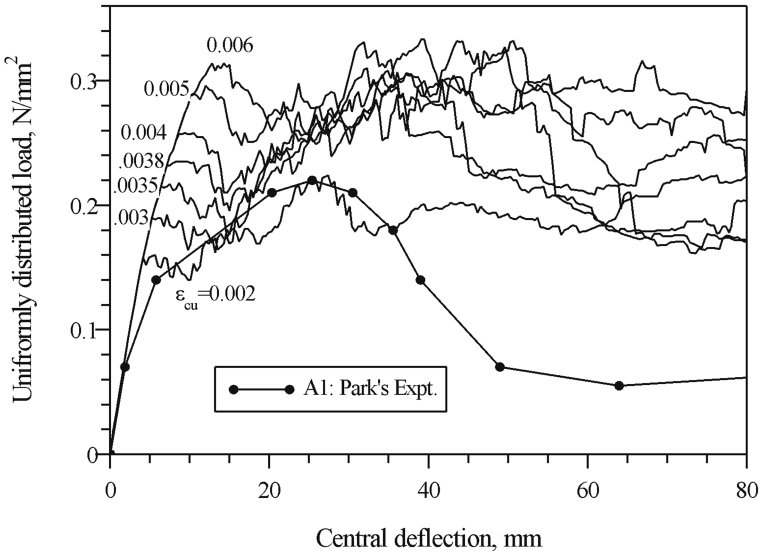

Fig. 6(c) Simulation of Park's slab A1 under DC

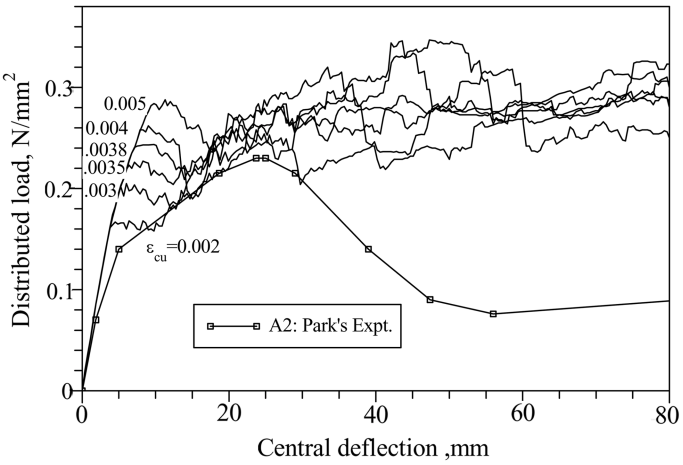

Fig. 6(d) Simulation of Park's slab A2 under DC

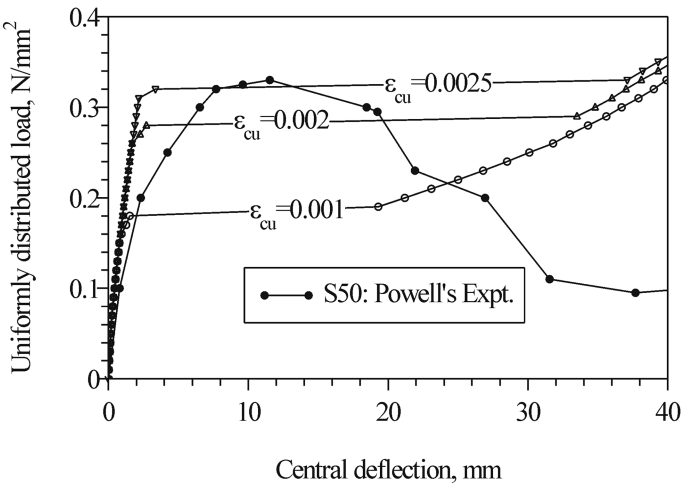

Fig. 7(a) Simulation of Powell's slab S50 under LC

However, in all simulation cases the deflection factor, (d_f, referred to under 'Ratio' in Tables 3 and 4), which relates the experimental to predicted displacement, is noted to have consistent values, which can conveniently be represented by a mean value, for each ε_{cu} value used. The summary of the basic simulation is presented in Table 5.

The LC strategy simulation is much easier to implement than the DC simulation strategy, as the DC simulation requires a preliminary determination of prescribed displacements, simulating the deflected shape of the slabs under distributed load. The direct predictions contained in the next section of this paper adopt the LC strategy, with a ε_{cu} value of 0.0025 for fully clamped slabs.

5. Direct simulation of previous tests

To test the reliability of the computational conditions and fixed concrete model parameter values

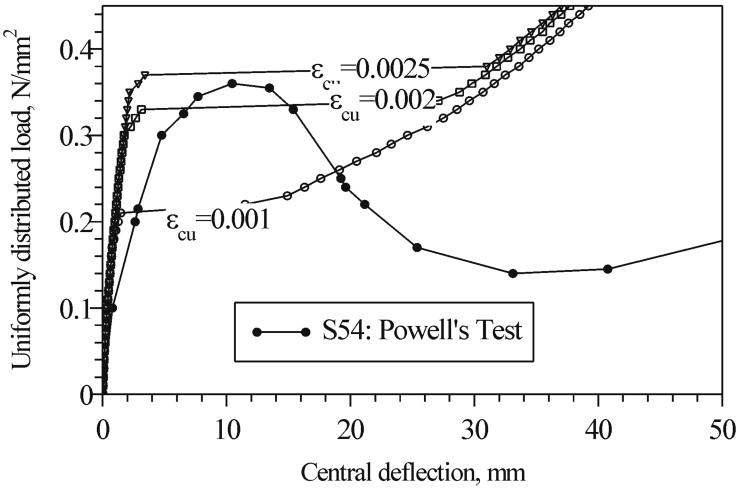

Fig. 7(b) Simulation of Powell's slab S54 under LC

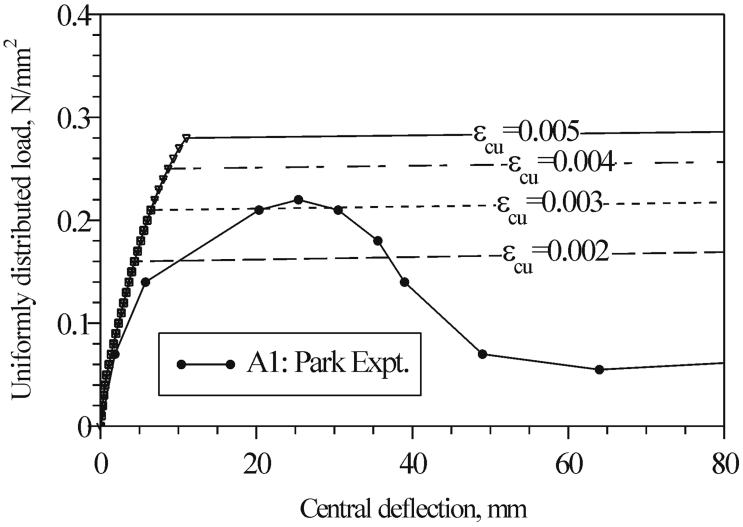

Fig. 7(c) Simulation of Park's slab A1 under LC

established from basic finite element simulation and parametric studies, the direct simulation of 42 other fully clamped slabs, tested by Powell (1956), Park (1964), Hung & Nawy (1971), Niblock (1986), Moy and Mayfield (1972), Keenan (1969), Skates (1986) and Wood (1961), are carried out.

5.1. Support conditions

The 42 slabs can be categorised into two classes. These are: Class I - Fully clamped slabs with lateral restraints, and Class II - Fully clamped with partial lateral restraint. The tests of Powell (1956), Park (1964), Keenan (1969), Niblock (1986) and Moy and Mayfield (1972), and Wood (1961) all fall into Class I. The rigid restraints at the supports were achieved by clamping the slabs from top using steel

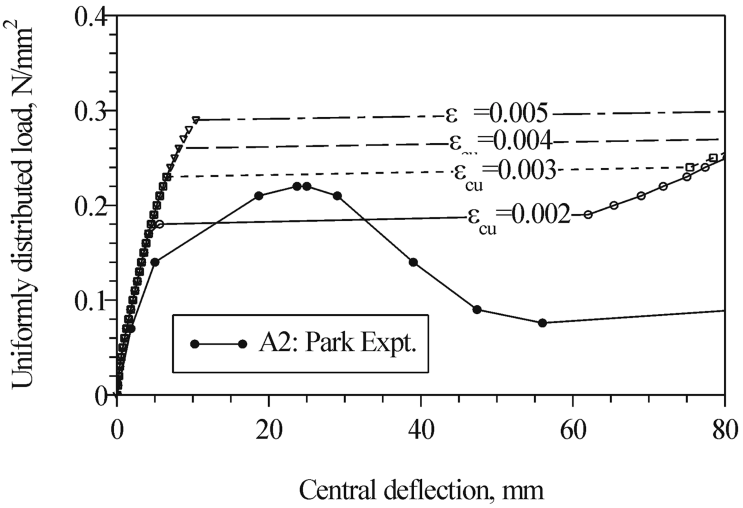

Fig. 7(d) Simulation of Park's slab A2 under LC

Table 4(a) Comparison of DC simulation with Park's (1964) experiment

Slab No.	Experiment		FE simulation (**DC**)				FE simulation (**DC**)			
	Load*	Defl. (mm)	Load*	Def. (mm)	**Ratio**[#] Load	Defl.	Load*	Def. (mm)	**Ratio**[#] Load	Defl.
A1	0.22	25.0	0.26	9.80	0.85	2.55	0.221	9.76	0.995	2.56
A2	0.22	23.5	0.26	9.20	0.85	2.55	0.232	9.25	0.948	2.54
A3	0.26	22.86	0.29	10.0	0.90	2.30	0.253	10.0	1.03	2.29
A4	0.26	18.63	0.30	8.0	0.87	2.34	0.275	7.85	0.945	2.37
				Mean	0.87	2.43			0.98	2.44
			ε_{cu} = 0.004, d_f = 2.43				**ε_{cu} = 0.0035, d_f = 2.44**			

*Load (in N/mm^2) # Ratio of experimental to finite element values

Table 4(b) Comparison of LC simulation with Park's (1964) experiment

Slab No.	FE simulation **(LC)**			
	Load*	Defl. (mm)	**Ratio**[#]	
			Load	Defl.
A1	0.205	7.37	1.07	3.39
A2	0.21	7.22	1.04	3.25
A3	0.25	7.35	1.04	3.11
A4	0.285	6.05	0.91	3.08
		Mean	**1.02**	**3.21**
	ε_{cu} = 0.0025, d_f = 3.21			

*Load (in N/mm^2) # Ratio of experimental to finite element values

Table 5 Summary of basic simulation

Test	Displacement Control (DC) strategy			Load Control (LC) strategy		
	ε_{cu}	Load ratio	d_f	ε_{cu}	Load ratio	d_f
Powell (1956)	0.0045	1.026	2.37	0.0025	0.953	3.32
Park (1964)	0.004	0.87	2.43	0.0025	1.02	3.21
	0.0035	0.98	2.44			

sections and also providing restraint against horizontal movements at the edges. This could be by means of a heavily reinforced concrete structure surrounding the test slab (Wood 1961), thus preventing horizontal movement. A typical Class I support condition is shown schematically in Fig. 8(a).

The test slabs of Hung and Nawy (1971) fall into Class II, where the restraint at the supports was only provided by the clamping action of the top steel channel to the main support frame, and no restraint against horizontal movement was provided at the edges of the slab. Such cases of partial restraint in slabs leads to a relatively lower failure loads and higher central deflections, when compared to those tests (in Class I), where rigid restraint was present. A typical Class II support condition is shown in Fig. 8(b).

5.2. Slab details and finite element mesh

The details of the slabs in the two classes are presented in Tables 6 (a & b). The slabs represent a wide range of aspect ratios, breadth to depth ratios, percentage of reinforcement, concrete compressive strengths and steel yield strengths. The reinforcement pattern in these slabs is identical to those of Powell's slabs, used in the basic simulation, with equal isotropic reinforcement at the top and bottom. The load control strategy, with an ε_{cu} value of 0.0025 as identified from the basic simulation process, is adopted for the direct prediction in this section.

For the rectangular slabs, a quarter section is idealised with 8 elements as shown in Fig. 3a and for square slabs, a quarter section is idealised with 9 elements as shown in Fig. 9. The discretisation through the depth of the steel and concrete into layers is also similar to that adopted for the basic simulation, as shown in Fig. 3(c).

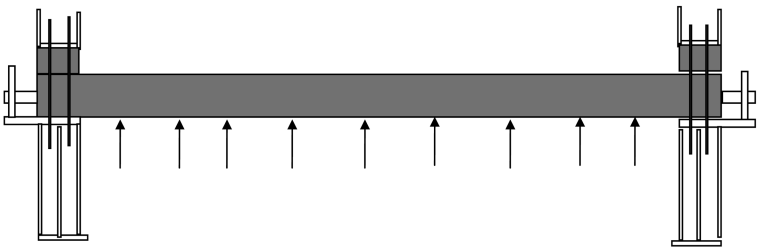

Fig. 8(a) Typical Class I support conditions Powell (1956) & Park (1964)

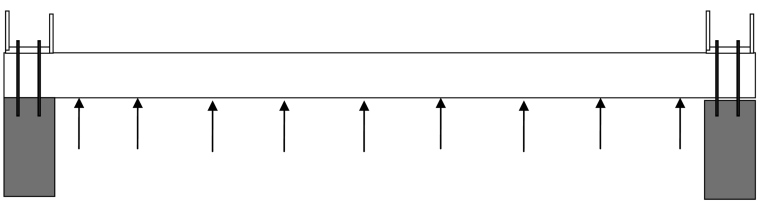

Fig. 8(b) Typical Class II support conditions Hung & Nawy (1971)

Table 6(a) Details of Class I slabs

Slab No.	L_y/L_x	L_x/h	d mm	% of Steel	f_y N/mm^2	f'_c N/mm^2
Powell's (1956) slabs (914.4x522.5x32.7mm)						
S46	1.75	16	25.2	0.25	211	40.1
S47		〃	〃	0.25	211	44.8
S55	〃	〃	〃	0.71	211	36.8
S58				0.97	255.2	40.0
S63	〃	〃	〃	1.53	255.2	36.3
S48	〃	〃	--	0.0	-	41.0
S53	〃	〃	--	0.0	-	37.6
S56	〃	〃	--	0.0	-	38.2
S57	〃	〃	--	0.0	-	39.6
S60	〃	〃	--	0.0	-	39.7
S64	〃	〃	--	0.0	-	39.7
Slabs tested by Wood (1961) (1727.2x1727.2x57.2mm)						
FS12	1.00	30.2	46.4	0.26	233	32.6
FS13	〃	〃	〃	0.26	233	26.5
FS14	〃	〃	--	0.00	--	28.6
Slabs tested by Keenan (1969): 1828.8x1828.8x76.2 mm						
3S1	1.00	24	58.2	0.82	326.9	24.5
3S2	〃	〃	--	0.00	--	28.6
3S3	〃	〃	58.2	0.82	326.9	28.4
3S4	〃	〃	〃	0.82	326.9	22.8
4.75S1	1.00	15.2	93.3	0.89	342.1	21.9
Slabs tested by Moy and Mayfield (1972) (1530 x1530 x5 0mm)						
FEA1	1.00	30.6	38.0	0.49	386.0	31.7
FEA4	1.50	〃	〃	0.49	386.0	31.7
FEA7	2.00	〃	〃	0.49	386.0	31.7
Slabs tested by Skates (1986) (950 x 950 x 50mm)						
S3	1.00	19.0	38.0	0.337	500.0	56.2
Slabs tested by Niblock (1986) (950 x 950 x 50.0mm)						
S1	1.00	19.0	--	0.00	--	42.3
S2	1.00	19.0	38.0	0.258	510.0	37.0
S4	1.00	19.0	38.0	0.516	510.0	30.4
Slabs tested by Park (1956) (1524x1016x50.8mm)						
D1	1.50	20		0.0		34.6
D2	〃	26.67		0.0		34.2
D3	〃	40.80		0.0		35.5
D4	〃	39.53		0.0		30.6
D5	〃	40.32		0.0		24.5

Table 6(b) Details of Class II slabs

Slab No.	L_y/L_x	L_x/h	d mm	% of Steel	f_y N/mm^2	f'_c N/mm^2
Slabs tested by Hung & Nawy (1971) (1651x1194x63.5mm)						
C1-1	1.00	26	50.8	0.58	471.0	38.6
C1-2	〃	〃	〃	0.36	475.2	38.6
C1-3	〃	〃	〃	0.28	471.0	33.1
C1-4	〃	〃	〃	0.25	474.5	38.6
C1-5	〃	〃	〃	0.36	475.2	34.4
C1-6	〃	〃	〃	0.38	471.0	34.4
C1-7	〃	〃	〃	0.58	286.9	39.0
C4-1	1.38	18.8	50.8	0.58	286.9	33.0
C4-2	〃	〃	〃	0.28	471.0	39.8
C4-3	〃	〃	〃	0.58	471.0	39.8
C4-4	〃	〃	〃	0.36	475.2	34.6
C4-5	〃	〃	〃	0.38	471.0	34.6

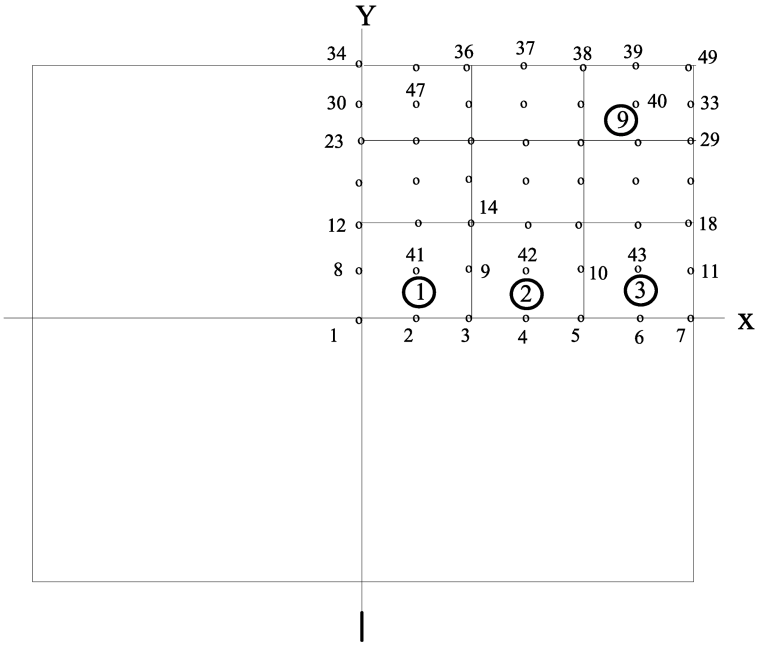

Fig. 9 Idealisation of square slabs

6. Results and comparative study

6.1. Comparison of peak loads

Table 7 compares the peak loads obtained from the experiments with those obtained from direct finite element predictions. Apart from two cases where the experimental values were not reliable,

the mean ratios of experimental to finite element predicted peak load values, for all the tests considered (from various researchers), ranged from 0.872 to 1.175, with an overall average ratio of 0.9698 and a standard deviation of 0.117. This shows a reasonably good agreement.

6.2. Comparison of central deflections

Table 8 compares the values of the central deflections obtained from the experiments with those obtained from direct finite element predictions. Only 22 of the slabs are involved in this comparison as the deflection values for the rest were not recorded in the available literature. The ratios of the experimental to predicted deflections are calculated for the slabs in Classes I and II, and the mean ratio is computed for each class separately.

The deflection ratios for Class II slabs are found to be higher (averaging 5.24) for the case of the 12 partially restrained slabs of Hung and Nawy (1971), than those of the 10 rigidly restrained slabs in Class I, from different authors, (averaging 3.495). This confirms the dependency of deflection factors on the degree of restraint. The displacement factor (d_f : 3.495) derived from the direct simulation of 10 rigidly restrained slabs is found to be in fairly good agreement to the displacement factor (d_f : 3.32), derived from the basic simulation of similar rigidly restrained slabs of Powell (1956). The difference in the deflection factors is probably due to the fact that no two experimental test set-ups can be identically the same, and the ideal fixity (100%), assumed in finite element analysis can only be partially achieved in real life.

The reliability of the finite element system, employed for the direct prediction is also illustrated, even in the ratios returned for the partially restrained slabs in Class II (Table 8). The consistency of the ratios (ranging from 4.40 to 6.2, and averaging at 5.24), suggests that if the restraints were to be in the same class as that of Class I, comparable results would be obtained.

6.3. Summary of basic and direct simulation

A summary of the load and deflection ratios obtained from the basic and direct simulation is shown in Table 9. The excellent agreement between the two sets of values confirms the reliability of the finite element system developed, and its credibility for any future predictions carried out for any arbitrary fully clamped reinforced concrete slabs.

7. Membrane action

The membrane action due to in-plane forces, inherent in the class of slabs under consideration but which the yield line analysis cannot account for, is illustrated in Table 10. The table re-states the experimental and finite element predicted loads, as well as equivalent predictions based on the yield line method. The yield line analysis was based on the use of a moment per unit width (m), calculated from the equation first proposed by Whitney (1937) and used in Leet & Bernal (1996), conforming to 1995 ACI code. This is expressed as:

$$m = \rho f_y d^2 (1 - 0.59 \rho f_y / f'_c) \tag{5}$$

where ρ is the reinforcement ratio, f_y is the steel yield strength and f'_c is the concrete uniaxial

Table 7 Comparison of experimental and predicted loads

Slab No.	Expt. load; N/mm^2	F.E. load;N/mm^2	Ratio of expt. to F.E.	
Powell (1956)				Average
S46	0.31	0.29	1.06	
S47	0.27	0.29	0.93	
S55	0.379	0.36	1.05	
S63	0.464	0.52	0.89	
S48	0.254	0.25	1.016	0.99
S53	0.289	0.25	1.15	
S56	0.259	0.25	1.03	
S57	0.21	0.24	0.875	
S60	0.224	0.24	0.933	
S64	0.241	0.25	0.964	
Hung & Nawy (1971)				
C1-1	0.16	0.16	1.00	
C1-2	0.13	0.15	0.87	
C1-3	0.1214	0.15	0.81	
C1-4	0.1214	0.15	0.81	
C1-5	0.133	0.15	0.89	
C1-6	0.1397	0.15	0.931	0.872
C1-7	0.1611	0.16	1.006	
C4-1	0.214	0.26	0.813	
C4-2	0.19	0.24	0.792	
C4-3	0.222	0.27	0.82	
C4-4	0.21	0.25	0.84	
C4-5	0.201	0.23	0.88	
Park (1964) D1	0.17	0.175	0.97	
D2	0.089	0.093	0.96	
D3	0.032	0.030	1.067	0.97
D4	0.29	0.032	0.91	
D5	0.0265	0.28	0.95	
Niblock (1986) S1	0.45	0.32	1.40*	
S2	0.40	0.34	1.17	1.175
S4	0.45	0.38	1.18	
Moy & Mayfield (1972)				
FEA1	0.091	0.10	0.91	
FEA4	0.05	0.07	0.72*	0.875
FEA7	0.0502	0.06	0.84	
Keenan (1969) 3S1	0.22	0.20	1.10	
3S2	0.162	0.16	1.02	
3S3	0.238	0.21	1.13	1.10
3S4	0.221	0.20	1.10	
4.75S1	0.58	0.49	1.18	
Skates (1986)				
S3	0.35	0.31	1.13	
Wood (1961) FS12	0.116	0.105	1.10	
FS13	0.085	0.095	0.895	0.94
FS14	0.065	0.08	0.82	
			Mean: 0.9698 Std. Dev.: 0.117	

*experimental values are not reliable and are not considered in the calculation of mean

Table 8 Comparison of experimental and predicted deflections

Slab No.	Experimental central deflection; mm	FE predicted deflection, mm	Ratio of expt. to predicted defl.
	Rigidly restrained slabs (Class I) d_f		
Park (1964)			
D1	21.0	5.76	3.64
Niblock (1986) S1	22.0	6.50	3.38
S2	14*	6.70	2.08*
S4	20.0	5.54	3.61
Moy & Mayfield (1972)			
FEA1	38.0	11.30	3.36
Keenan (1969) 3S1	38.6	10.24	3.76
3S2	25.4*	13.25	1.92*
3S3	34.54	11.2	3.08
3S4	34.29	9.0	3.81
4.75S1	23.37	7.02	3.32
			Mean: 3.495
	Partially restrained slabs (Class II)		d_f
Hung & Nawy (1971)			
C1-1	56.4	10.69	5.27
C1-2	50.8	9.19	5.52
C1-3	56.0	10.31	5.43
C1-4	52.0	10.30	5.08
C1-5	51.8	9.30	5.56
C1-6	54.0	9.21	5.86
C1-7	52.0	11.36	4.58
C4-1	47.0	7.56	6.2
C4-2	41.0	7.66	5.35
C4-3	39.6	9.00	4.40
C4-4	43.0	8.95	4.80
C4-5	43.0	8.90	4.83
			Mean : 5.24

*experimental values are not reliable and are not considered in the calculation of mean

Table 9 Summary of basic and direct simulations

Type	Ratio of expt. to predicted loads	Ratio of expt. to pred. Defl. (Defl. factor, d_f)
Basic finite element simulation	0.94	3.32
Direct simulation of 42 slabs	0.9698	3.495*

*Ratios for Class I slabs only are considered

compressive strength. This expression has been shown to be most accurate for under-reinforced sections (i.e., for reinforcement ratios less than that required for balanced failure). From Table 10 it is noted that the yield line theory under-predicts failure loads by a factor as much as between 7.67 and 8.2 in comparison with experimental tests and finite element predictions respectively.

8. Practical applications of membrane action simulation

Achieving reliable predictions for a class of slabs subjected to membrane action in concrete structures based on fixed parameter values, opens the avenue for numerous practical applications. Hundreds of 'computer model slabs' of various geometric and strength properties could be analysed with greater confidence to provide a database of peak load and corresponding displacements values. This database could be used as the basis for the development of charts and equations, which can be used for an easy and quick peak-load and displacement determination, for any proposed reinforced concrete slab structure. This is done without the need for extensive finite element analysis at the time the information is required, or the need for physical testing of a typical slab, which will be time consuming, considering the fact that the structure has to be cured for at least 28 days before testing. The database can also be used as a basis for the development of a knowledge based system.

To illustrate the possibility for practical applications highlighted above, a series of predictions was carried out for typical fully clamped 'computer model slabs' where membrane action is significant, with different geometric and strength properties as shown in Table 11. A total of 864 model slabs were analysed and the information obtained from these were used in the development of charts. These charts were developed for various characteristic strengths of concrete and steel, width to depth ratios, aspect ratios and reinforcement ratios and and a typical one is shown in Fig. 10.

The data points in Fig. 10 have been joined by polynomials of the 3rd degree, thus each curve has a unique equation, which in itself can be used as a tool for direct strength prediction, and can also be useful in a computer aided design process. The concrete cylinder strength (f'_c), steel yield strength (f_y) and aspect ratio of slab are shown at the top of the chart. The prediction curves have been developed for reinforcement ratios varying from 0.2 to 1.5%, which are indicated on the charts. The design loads are expressed as a function of Breadth/depth ratios (varying from 15 to 40). In Fig. 10, the estimation of loads for slabs having breadth to depth ratios of 17 and 20, and reinforcement ratios (in %), of 0.5 and 1.25, are shown by lines with arrows. For predicting the failure load for a slab with reinforcement ratio of 1.25%, a linear interpolation between 1.0 and 1.5% is adopted.

Detailed assessment of the charts has been done in which predictions based on the charts were compared with both the direct finite element predictions and experiments. The mean value of the ratio of chart predicted loads to direct finite element prediction, was found to be 0.984, confirming that the charts are almost as accurate as direct finite element predictions. The ratio of the experimental to chart predicted loads was also found to be 0.9698, which is consistent with that obtained from the direct finite element simulation of 42 experimental slabs of different authors, as shown in Table 7.

Current researches (Alan Hon, *et al.* 2001, Das 2001, Eyre 1997, Peel-Cross, *et al.* 1998, Taylor, *et al.* 1998a, 1998b, Rankin, *et al.* 1999, Taylor 2000, Salim and Sebastian 2003, Huang, *et al.* 2003a, 2003b) on building and bridge structures reflect the importance of membrane action in slabs or decks with normal and high strength concrete and under various loading conditions including fire. The simulation of membrane action in concrete slabs through optmisation of a concrete model

Table 10 Comparison of experimental with FE and yield line loads

Slab No.	Experimental load; N/mm^2	FE load; N/mm^2	Yield line method	Ratio of Expt/yield	Ratio of FE /Yield	Ratio of Expt/FE
Powell (1956)						
S46	0.31	0.29	0.0378	8.20	7.67	1.06
S47	0.27	0.29	0.0379	7.12	7.65	0.93
S50	0.33	0.32	0.0676	4.88	4.73	1.03
S54	0.36	0.37	0.106	3.40	3.49	0.973
S55	0.379	0.36	0.1056	3.59	3.41	1.05
S59	0.35	0.39	0.172	2.03	2.26	0.897
S62	0.426	0.49	0.266	1.60	1.84	0.87
S63	0.464	0.51	0.264	1.76	1.93	0.91
S58	0.342	0.38	0.172	1.99	2.21	0.90
Hung& Nawy (1971)						
C1-1	0.16	0.16	0.119	1.345	1.345	1.00
C1-2	0.13	0.15	0.076	1.71	1.97	0.87
C1-3	0.1214	0.15	0.0585	2.07	2.56	0.81
C1-4	0.1214	0.15	0.053	2.29	2.83	0.81
C1-5	0.133	0.15	0.0755	1.76	1.90	0.89
C1-6	0.1397	0.15	0.0788	1.77	1.90	0.931
C1-7	0.1611	0.16	0.074	2.17	2.16	1.006
C4-1	0.214	0.26	0.1053	2.03	2.47	0.813
C4-2	0.19	0.24	0.0843	2.25	2.85	0.792
C4-3	0.222	0.27	0.1706	1.30	1.58	0.82
C4-4	0.21	0.25	0.1082	1.94	2.31	0.84
C4-5	0.201	0.23	0.1072	1.875	2.14	0.88
Niblock (1986)						
S2	0.40	0.34	0.099	4.04	3.43	1.17
S4	0.45	0.38	0.192	2.34	1.98	1.18
Moy & Mayfield (1972)						
FEA1	0.091	0.10	0.054	1.69	1.85	0.91
FEA4	0.05	0.07	0.0383	1.30	1.83	0.72*
FEA7	0.0502	0.06	0.032	1.57	1.88	0.84
Keenan (1969)						
3S1	0.22	0.20	0.1219	1.805	1.64	1.10
3S2	0.162	0.16	--			1.02
3S3	0.238	0.21	0.123	1.935	1.71	1.13
3S4	0.221	0.20	0.1212	1.823	1.65	1.10
4.75S1	0.58	0.49	0.3492	1.661	1.40	1.18
Skates (1986)						
S3	0.35	0.31	0.127	2.76	2.44	1.13
Wood (1969)						
FS12	0.116	0.105	0.0208	5.577	5.04	1.10
FS13	0.085	0.095	0.0207	4.11	4.59	0.895

*experimental values are not reliable and are not considered in the calculation of mean

Table 11 Variable values used for computer-model slabs

Aspect ratio L_y/L_x	Breadth to depth ratio L_x/h	Concrete cylinder strength f'_c N/mm^2	Steel yield strength, f_y N/mm^2	Percentage of steel, ρ (%)
2.0, 1.5, 1.0	15, 20, 25, 30, 35, 40	25, 30, 40, 60	250, 460, 550	0.2, 0.5, 1.0, 1.5

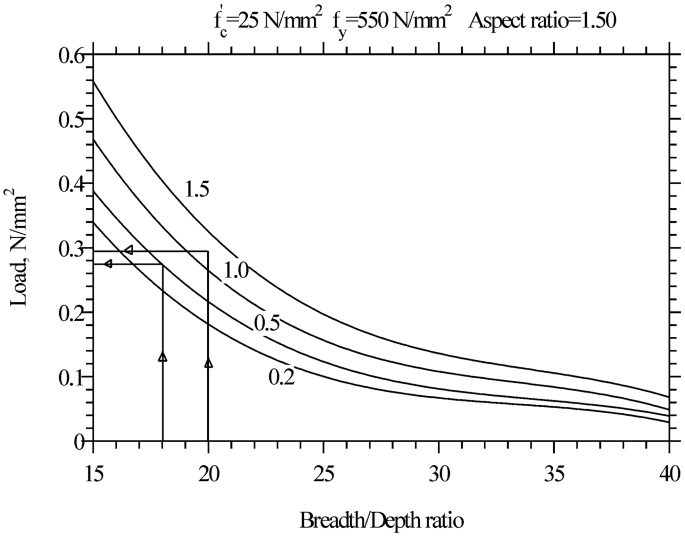

Fig. 10 Typical chart showing the prediction of load

presented in this paper is the first step towards comprehensive research on floor slabs in buildings and bridge decks under various loading conditions including fire, and research is currently ongoing in these directions.

9. Conclusions

The development of compressive membrane action in slabs in building and bridge structures due to the presence of horizontal end restraints significantly increases their load carrying capacity. The incorporation of strength enhancement due to membrane action can lead to the economical design of such structures. This study illustrates the finite element simulation of membrane action in reinforced concrete slabs through optmisation of a concrete model and numerical conditions. The study involves a parametric optimisation process, used to identify a set of fixed model parameter values and computational conditions, by the simulation of tests on 8 fully clamped slabs. The confidence derived from this preliminary process led to the further ultimate load predictions of 42 previously tested slabs, with the fixed parameter values. This direct simulation process under load control gave an average value of 0.9698 for the ratio of the experimental to finite element predicted strengths. A deflection factor d_f was also established from the basic simulation, which subsequent direct prediction of class I slabs (fully clamped with lateral restraints) confirms as credible. The study clearly demonstrates that reliable finite element predictions can be carried out for the strengths

and deflections of this class of slabs with reasonable accuracy. The weakness of the yield line method of analysis, in not accounting adequately for membrane action has also been demonstrated, especially for slabs where significant in plane forces are present at the edges.

Many practical applications can be found for the proposed reliable finite element procedure. Developed charts and equations will allow a quick and fairly accurate strength determination. Development of expert and knowledge based systems are also possible, as well as applications to neural networks.

Another avenue for application of the proposed finite element procedure is in the design of reinforced concrete structures. Existing design practice use codes which adopt either partial or global factors of safety for the applied loads and materials, and which to varying degrees, (even for the limit state design methods), limit the structural performance to within the elastic range. This could be because in most cases, the method of analysis that preceeds the design does not account adequately for the nonlinearities that are inherent in concrete structures, thus the design tends to be overly conservative. Structural integrity is well known to be preserved even when the structure is in the nonlinear range. Since accurate determination of the peak strength and displacement have been demonstrated as achievable with finite element modelling, the designer is able to peg a point in the nonlinear range of the loading curve, when the structure may be assumed to have failed. Fixing such a point on the loading curve is synonymous to the imposition of a global factor of safety whose choice would lead to optimum use of material while not compromising safety requirements. This approach will lead to reduction in construction costs. Charts and equations discussed, when used with an appropriate factor of safety, can be adapted for such reinforced concrete structural design.

The optimised concrete model and proposed finite element procedure can be used to simulate membrane action in slabs in buildings and bridges with varying structural configurations subjected to various loading conditions and research is currently ongoing in these directions.

References

Alan Hon, A., Geoff Taplin, G. and Riadh Al-Mahaidi, R. (2001), "Compressive membrane action in reinforced concrete one-way slabs", *The Eighth East Asia-Pacific Conference on Structural Engineering and Construction*, 5-7 December, Nanyang Technological University, Singapore, Paper No.1276, 8.

Braestrup, M. W. (1980), "Dome effects in RC slabs: rigid plastic analysis", *J. Struct. Div. ASCE*, **106**(ST6), 1237-1253.

Cedolin, L. and Deipoli, S**.** (1977), "Finite element studies of shear-critical R/C beams", *J. Eng. Mech. Div., ASCE*, **103**(EM3), 395-410.

Das, S. K. (2001), "Compressive membrane action in circular reinforced concrete slabs", Masters dissertation, Dept. Engineering, University of Cambridge, UK.

Eyre, J. R. (1997), "Direct assessment of safe strengths of RC slabs under membrane action", *J. Struct. Eng.*, **123**(10), 1331-1338.

Huang, Z., Burgess, I. W. and Plank, R. J. (2003a), "Modeling membrane action of concrete slabs in composite buildings in fire. I: theoretical development", *J. Struct. Eng.*, **129**(8), August, 1093-1102.

Huang, Z., Burgess, I. W. and Plank, R. J. (2003b), "Modeling membrane action of concrete slabs in composite buildings in fire. II: validations", *J. Struct. Eng.*, **129**(8), August, 1103-1112.

Hung, T. Y., Nawy, E. G. (1971), "Limit strength and serviceability factors in uniformly loaded, iso-tropically reinforced two way slabs", *ACI, Detroit*, ACI SP-30, 301-324.

Johansen, K. W. (1962), *Yield Line Theory*, Cement and Concrete Association, London.

Keenan, W. A. (1969), "Strength and behaviour of restrained reinforced concrete slabs under static and dynamic loadings", Technical Report R621, U.S. Naval Civil Engineering Laboratory, Port Hueneme, California, April, 133.

Kirkpatrick, J., *et al.* (1984**),** "Strength evaluation of M-beam bridge deck slabs", *The Structural Engineer*, **62B** (3), Sept., 60-68.

Kupfer, K. H., Hilsdorf, K. H. and Rush, H. (1969), "Behaviour of concrete under biaxial stresses", *Proceedings, ACI*, **66**(8**)**, 656-666.

Leet, K. M. and Bernal, D. (1996), *Reinforced Concrete Design*, 3rd Edition, Mcgraw-Hill, New York.

Moy, S. S. J. and Mayfield, B. (1972), "Load-deflection characteristics of rectangular reinforced concrete slabs", *Mag. Conc. Res.*, **24**(81).

Niblock, R. A. (1986), "Compressive membrane action and the ultimate capacity of uniformly loaded reinforced concrete slabs", Ph. D. thesis, The Queen's University of Belfast, UK.

Ockleston, A. E. (1955), "Load tests on a three storey reinforced concrete building in johannesburg", *The Struct. Eng.*, **33**, 304-322.

Owen, D. R. J. and Figueiras, J. A. (1983), "Anisotropic elasto-plastic finite element analysis of thick and thin plates and shells", *Int. J. Num. Meth. Eng.*, **19**, 541-566.

Owen, D. R. J. and Figueiras, J. A. (1984), "Ultimate load analysis of reinforced concrete plates and shells including geometric nonlinear effects", *Finite Element Software for Plates and Shells*, by E. Hinton and D.R.J. Owen, Pineridge Press, London.

Owen, D. R. J. and Hinton, E. (1980), *Finite Elements in Plasticity- Theory and Practice*, Pineridge Press, Swansea, UK.

Park, R. (1964a), "The ultimate strength and long-term behaviour of uniformly loaded, two-way concrete slabs with partial lateral restraint at all edges", *Mag. Conc. Res.*, **16**(48), 139-152.

Park, R. (1964b), "Ultimate strength of rectangular concrete slabs under short-term uniform loading with edges restrained against lateral movement", *Proc. the Institution of Civil Engineers*, **28**, 125-150.

Park, R. (1965), "The lateral stiffness and strength required to ensure membrane action at the ultimate load of a reinforced concrete slab-and-beam floor", *Mag. Conc. Res.*, **17**(50) 29-38.

Peel-Cross, R. J., Gilbert, S. G., Rankin, G. I. B. and Long, A. E. (1998), "Arching action in composite metal deck concrete slabs", *Proc. Third Cardington Conference*, Whole Building Research: the Latest Developments, BRE, 26-27 November. pp. 30-36.

Powell, D. S. (1956), "Ultimate strength of concrete panels subjected to uniformly distributed loads", Cambridge University Thesis, England.

Rankin, G. I. B., *et al.* (1991), "Compressive membrane action strength enhancement in uniformly loaded laterally restrained slabs", *The Structural Engineer*, **69**(16), 287-295.

Rankin, G. I. B., Taylor, S. E. and Cleland, D. J. (1999), "A guide to compressive membrane action in bridge deck slabs", *Design Guide for the Concrete Bridge Development Group*, British Cement Association, December.

Salami, A. T. (1994), "Equation for predicting the strength of fully clamped two-way reinforced concrete slabs", *Proc. Inst. Civ. Engr. Structs. & Bldgs*, **104**, 101-107.

Salim, W. and Sebastian, W. M. (2003), "Punching shear failure in reinforced concrete slabs with compressive membrane action", *ACI Struct. J.*, **100**(4), 471-479.

Skates, A. S. (1986), "Development of a design method for restrained concrete slab systems subject to concentrated and uniform loading", Ph. D. Thesis, The Queen's University of Belfast, UK.

Taylor, S. E., Rankin, G. I. B. and Cleland, D. J. (1998a), "Compressive membrane action in high strength concrete bridge deck slabs", *Proce. 2nd International Symposium on Concrete under Severe Conditions*, Environment and Loading, CONSEC '98, Tromso, Norway, Norwegian Concrete Association, 21-24 June, **3**, 1704-1713.

Taylor, S. E. (2000), "Compressive membrane action in high strength concrete bridge deck slabs", Ph. D. thesis, Queen's University of Belfast, Jan.

Taylor, S. E., Rankin, G. I. B. and Cleland, D. J. (1998b), "High strength concrete bridge slabs with in-plane restraint", *Proce. British Cement Association Annual Conference*, Southampton, England, July.

Whitney, C. S. (1937), "Design of reinforced concrete members under flexure or combined flexure and direct compression", *J. American Conc. Inst.*, **33**, 483-498, March-April.

Wood, R. H. (1961), *Plastic and Elastic Design of Slabs and Plates*, Thames and Hudson, London, 344.

CC